OPEN ACCESS
IOP Publishing | Astro Ltd
Laser Physics Letters
Laser Phys. Lett. **18** (2021) 065401 (5pp)
https://doi.org/10.1088/1612-202X/abff49

Letter

High temporal contrast ultrashort pulses generated by nonlinear ellipse rotation in multipass cells

Viktor Pajer[1,*] **and Mikhail Kalashnikov**[1,2]

[1] ELI-ALPS, ELI-HU Non-Profit Ltd, Szeged, Hungary
[2] Max Born Institute for Nonlinear Optics and Short Pulse Spectroscopy, Berlin, Germany

E-mail: viktor.pajer@eli-alps.hu

Received 31 March 2021
Accepted for publication 23 April 2021
Published 20 May 2021

Abstract

The simultaneous nonlinear spectral broadening and temporal cleaning of ultrashort pulses by the combination of the multipass cell (MPC) technique and nonlinear ellipse rotation are proposed and investigated with numerical simulations. The performance of the gas-filled MPC is studied at 800 and 1030 nm central wavelengths with mJ energy level. The results indicate that at least 10^3 contrast enhancement is feasible with 50% internal efficiency while the beam quality is preserved during propagation. At the same time, nonlinear spectral broadening allows for a more than five-fold temporal compression. The technique is tested at 20 mJ energy and it is presumably suitable for the generation of high contrast, high energy few-cycle pulses, too.

Keywords: contrast, multipass cell, post-compression

(Some figures may appear in colour only in the online journal)

1. Introduction

Ultrashort laser pulses with high intensities are the basis of applications like high harmonic generation [1], ultrafast spectroscopy [2] or laser driven particle acceleration [3]. Nowadays, post-compression techniques based on nonlinear processes like self-phase modulation (SPM), are routinely applied to obtain few-cycle pulses [4]. Solid materials such as fused silica in a multiple plate configuration [5] as well as noble gases in a hollow core fibre [6] have been successfully used to achieve the required spectral broadening, and now both techniques are able to generate single-cycle pulses [7–9]. In the last few years, multipass cells (MPCs) have also attracted great interest because of the excellent output beam quality and high transmission [10–13]. Another great advantage of an MPC is that it is suitable for both solid materials and for gas-filled configurations. By using noble gases as nonlinear medium, it has been demonstrated that the post-compression of ps long pulses to the fs regime is feasible at mJ energy level [14, 15].

As the above mentioned post-compression techniques are able to deliver few-cycle pulses with TW peak power, temporal contrast has become highly important in applications, as the light preceding the main pulse, e.g. a pre-pulse can significantly affect the interaction properties. Consequently, nonlinear temporal filtering such as cross-polarized wave generation [16], plasma mirrors [17], nonlinear elliptical polarization rotation (NER) [18] or spectral filtering [19] are widely used in high peak power laser systems. NER is a promising technique since it exhibits high conversion efficiency [20] and in optical waveguides it provides excellent spatial

* Author to whom any correspondence should be addressed.

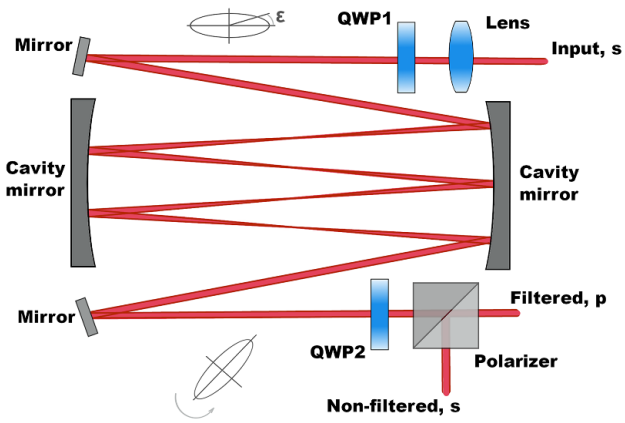

Figure 1. The proposed experimental setup for temporal cleaning. For clarity, only a few passes in the cell are presented. The polarization ellipse rotates during propagation. ε—the input ellipticity, QWP—quarter wave plate.

beam characteristics. Another great advantage is that temporal cleaning and nonlinear spectral broadening for post-compression can be performed at the same stage. NER in an air-filled cavity [21] applied for contrast improvement in Double chirped pulse amplification (CPA) laser systems [22] was demonstrated rather long ago. Because of the slow nonlinearity of air, no pulse shortening was demonstrated and since then no further investigations have been done to explore the possibilities of temporal cleaning in MPCs.

Here, we propose to utilize the noble gas-filled MPC post-compression technique combined with NER to generate temporally clean pulses with shortened pulse duration. We present possible arrangements with optimized parameters for different wavelengths and energy levels. Our results are obtained by using a 3D numerical model.

2. Numerical simulation

The nonlinear spectral broadening and temporal cleaning of ultrashort pulses were examined by simulations with a 3D numerical model based on the proposed experimental setup shown in figure 1. The input beam is always linearly polarized. The first quarter wave plate (QWP1) is rotated with an angle of $0 < \varepsilon < \pi/4$ relative to input polarization and thus it generates an elliptically polarized pulse which induces NER inside the cell during nonlinear propagation. With the help of QWP2, the temporal phase added by QWP1 is compensated and the polarizer at the output separates the temporally filtered and non-filtered components. The filtered pulses can be compressed afterwards.

Based on the scaling rules by Hanna *et al* [10], first the geometry of the cavity was determined. In each case, a confocal arrangement was simulated. The cavity length and the number of round trips were set to accumulate the required B integral slowly to avoid ionization or any space-time coupling. To see the applicability of the technique at different wavelengths, the parameters of both an Ytterbium (Yb) and a titanium sapphire (Ti:Sa) system were considered. The values are based on the two available sources at ELI-ALPS Institute. Table 1 summarizes the main parameters used in the simulations. Lower nonlinear index was required for the Ti:Sa system because it generates pulses with higher intensity than the Yb laser. This condition could be fulfilled either by considering a gas at low pressure or by choosing a medium with lower nonlinearity (e.g. neon). Preliminary investigations showed that the latter case is a better choice, presumably because dispersion also has a significant impact, especially in the case of high spectral bandwidth.

Table 1. Main parameters used in the simulation.

Cavity	Yb	Ti:Sa
Radius of curvature = length (mm)	600	300
Number of round trips	15	20
Beam waist (μm)	313	195
Gas	Argon	Neon
Input pulse		
Pulse duration, FWHM (fs)	230	30
Central wavelength (nm)	1030	800
Energy (mJ)	4	1

The propagation of pulses in the MPC was simulated in a similar way as described in [10] except that the propagation of two pulses with orthogonal linear polarization ($E_H(x,y,t)$ and $E_V(x,y,t)$) were considered simultaneously, in order to take into account the input elliptical polarization, a feature necessary to induce NER. This approach is similar to the case of radially polarized pulses [23]. The elliptical polarization induced by the QWP1 was modelled by adding the required temporal phase shift to $E_V(x,y,t)$. In the same way, at the output, this phase shift was subtracted to compensate the effect of the input wave plate. The input pulse was always Gaussian in space and time and the spot size was chosen to match the fundamental spatial mode of the cavity. Diffraction and dispersion were simulated in the Fourier domain, and pressure dependent refractive indices were taken into account using Sellmeier equations [24]. Reflection on the concave mirrors was modelled by adding a quadratic spatial phase. No losses were considered but they can be easily implemented into the model. The temporal range was limited to ± 0.5 ps due to the large number of sampling points required for proper resolution.

In the case of elliptical polarization, the nonlinear refractive index change [25, 26] in an isotropic material is

$$\Delta n_i = n_2 \left(|E_i(x,y,t)|^2 + 2/3\, |E_j(x,y,t)|^2 \right), \qquad (1)$$

and thus the induced nonlinear polarization takes the form of

$$P_i = n_2 \left[|E_i(x,y,t)|^2 + 2/3\, |E_j(x,y,t)|^2 \right] E_i(x,y,t) + 1/3\, \left[(E_i^*(x,y,t) E_j(x,y,t)\ ) E_j(x,y,t) \right], \qquad (2)$$

where n_2 is the pressure-dependent nonlinear refractive index for linear polarization, * denotes the complex conjugate and E_i and E_j represent the two orthogonal polarization components, respectively. Nonlinear propagation was calculated in the space-time domain taking into account SPM, self-steepening

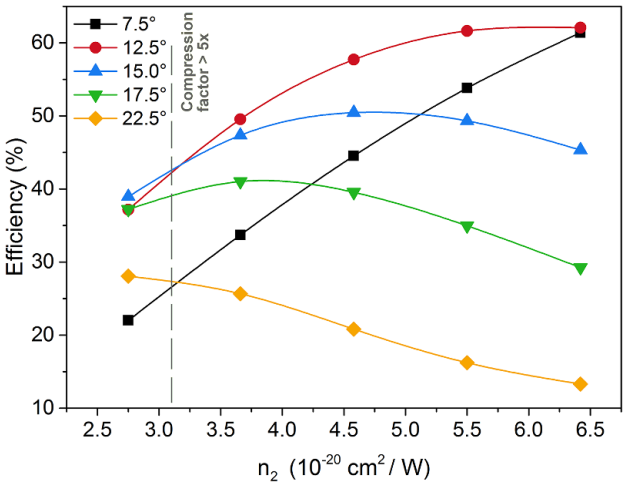

Figure 2. Efficiency as a function of n_2 and ellipticity. The dashed line indicates the limit for 5× compression.

(SS), self-focusing and cross-phase modulation. The equations were solved by using the split-step Fourier method.

3. Results

In gas-filled multipass cells, the experimentally obtained transmission can be higher than 85% [11]. The internal efficiency of NER, which is defined as the ratio of the filtered and input energies, is highly affected by polarization. In order to improve temporal contrast with the highest possible efficiency, first, we investigated the effect of the input polarization state. The ellipticity (ε) of the input polarization induced by QWP1 (figure 1) was varied in the range of 7.5°–22.5°. At the same time, the values of n_2 which are related to the indicated noble gases (table 1) at different pressures, were optimized to achieve a minimum compression factor of five. Experiments show that this can be easily obtained by using one MPC post-compression stage only [11, 12]. After these steps, the optimal case was selected where sufficient efficiency and compression were feasible at the same time. Simulations with linear polarization were also performed to compare the filtering effect. In these cases, the induced ellipticity given by QWP1 was set to 0°.

3.1. Yb system

For the Yb based laser system, argon was considered as a nonlinear medium. Figure 2 shows the efficiency as a function of the nonlinear refractive index. The vertical dashed line indicates the limit where the feasible compression becomes higher than five, thus the Fourier transform-limited (FTL) pulse duration is less than 46 fs in all cases. The curves show the strong dependence of the maximum attainable efficiency on the input ellipticity, and the trend is in agreement with what can be obtained from hollow core fibres [18].

It is clearly visible that more than 60% efficiency could be reached in the case of $\varepsilon = 12.5°$. Figure 3 shows the

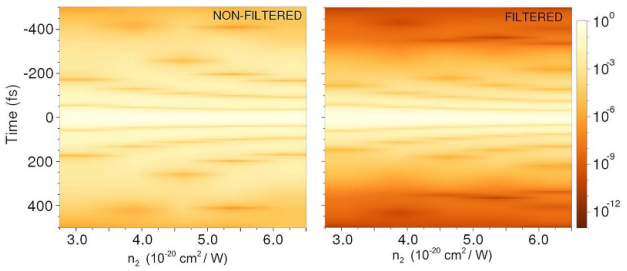

Figure 3. Evolution of the FTL temporal intensity profiles of the non-filtered (left) and filtered (right) components as a function of the nonlinear refractive index. The $\varepsilon = 12.5°$ is at the input.

evolution of the FTL temporal profiles. It can be seen that with 12.5° ellipticity, the filtered component has a much better contrast. On the other hand, the highest contrast enhancement in the ±200 fs range could be reached when $n_2 \leqslant 4.5 \times 10^{-20}$ cm^2 W^{-1}, which suggests that contrast and efficiency cannot be improved simultaneously. The reason presumably is that the filtered spectrum also becomes slightly modulated above a certain level and it is manifested in the contrast degradation of the compressed pulse.

Considering the results above, for this setup the optimal input parameters are: $\varepsilon = 12.5°$ and $n_2 = 3.66 \times 10^{-20}$ cm^2 W^{-1} (related to argon at 400 mbar pressure [27, 28]) with which 39.36 fs transform-limited pulse duration can be obtained with 49.55% internal efficiency. The overall accumulated on-axis B integral in this case was 14.8 radians, which is very close to the analytically estimated 16.2 radians [10].

Figures 4(a) and (b) show the output spatio-spectral and FTL spatio-temporal profiles of the filtered component. It can be seen that the beam quality is preserved and no space-time coupling is present. This means that the changes in polarization affect only efficiency but not the beam profile. In figure 4(c), the non-filtered component displays the typical strong spectral modulations caused by SPM—as in the case of linear polarization—while the filtered component has a more flattened shape. These features are reflected on the intensity profiles, too: with temporal filtering, the intensity of the side wings is reduced and in the ±250 fs temporal range 10^2–10^3 contrast enhancement could be obtained. The improvement is even better on a longer timescale.

3.1.1. Ti:Sa system. We also simulated the post-compression of pulses from a Ti:Sa system. The parameters of neon were used and optimized to achieve high efficiency and sufficient contrast improvement. Figure 5 shows the internal efficiency as a function of n_2. With values higher than 5.2×10^{-21} cm^2 W^{-1}, shorter than 6 fs pulse duration could be reached (vertical dashed line). Again, the polarization dependence is clearly visible.

The highest efficiency of more than 50% is related to the ellipticity value of $\varepsilon = 15°$. By comparing the evolution of the intensity profiles (figure 6) one can clearly see

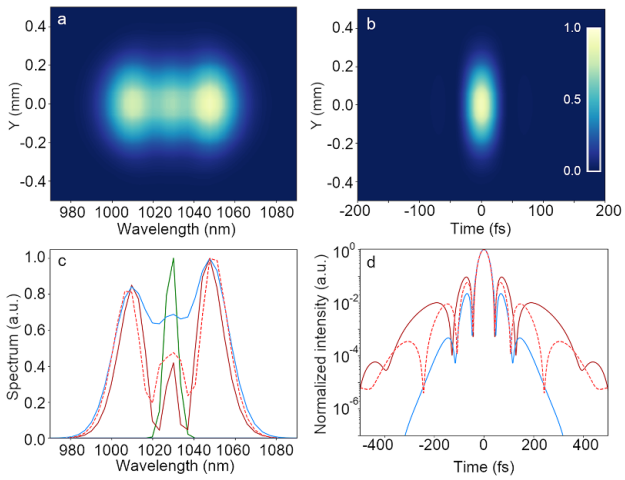

Figure 4. Output of the optimized setup. Space integrated spatio-spectral (a) and FTL spatio-temporal profiles (b) of the filtered component. Space integrated spectrum (c): green—input, dark red—non-filtered, blue—filtered and dashed—linear polarization. Space integrated FTL temporal profiles (d): red—non-filtered, blue—filtered, dashed—linear polarization.

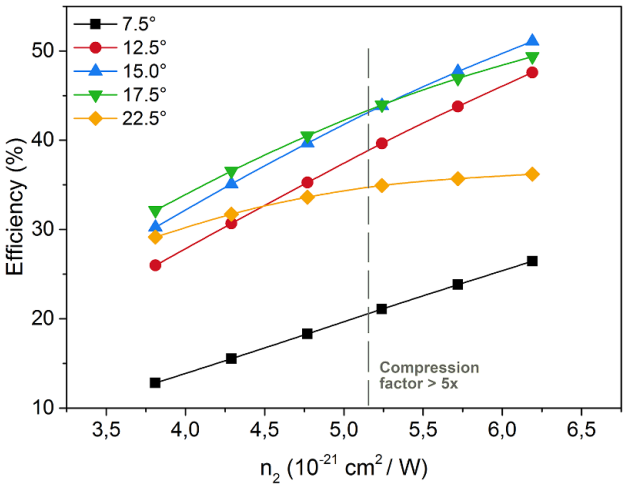

Figure 5. Efficiency as a function of n_2 and ellipticity. The dashed line indicates the limit for 5× compression.

that the filtered component has a much better contrast in each case.

Based on these results, $n_2 = 6.25 \times 10^{-21}$ cm^2 W^{-1} (related to neon at 650 mbar pressure) and $\varepsilon = 15°$ was considered as an optimal choice. The accumulated on-axis B integral in this case was 12.6 radians, which is in good agreement with the analytically estimated value of 11.96. The spectrum of the filtered component supports sub two-cycle pulses (5.16 fs FTL pulse duration). In figure 7 it can be seen that neither the spatio-spectral nor the FTL spatio-temporal profile show any distortions, which implies that the beam quality is preserved. The effect of NER on the spectrum is clearly visible: the filtered component has a smooth shape while the

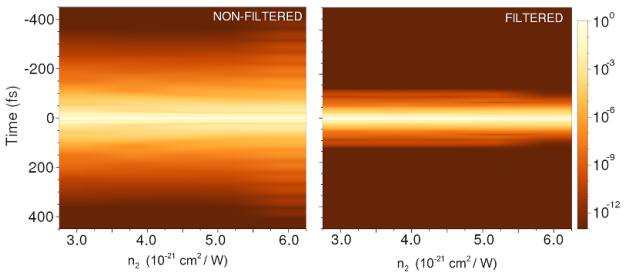

Figure 6. Evolution of the FTL temporal intensity profiles of the non-filtered (left) and filtered (right) components as a function of the nonlinear refractive index for the case of $\varepsilon = 15°$.

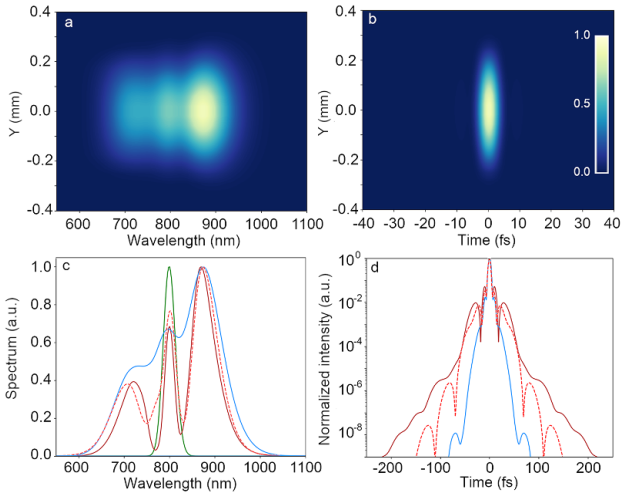

Figure 7. Output of the optimized setup. Space integrated spatio-spectral (a) and FTL spatio-temporal profiles (b) of the filtered component. Space integrated spectrum (c): green—input, red—non-filtered and blue—filtered and dashed—linear polarization. Space integrated FTL temporal profiles (d): red—non-filtered, blue—filtered and dashed—linear polarization.

non-filtered component has strong modulations just like with linear input polarization (figure 7(c)). The asymmetry of the pulse spectrum is a typical feature caused by SS. The FTL intensity profile shows (figure 7(d)) the benefit of the technique: >10^3 contrast enhancement could be obtained.

3.1.2. High energy Ti:Sa system. Theoretically, MPCs are suitable for the post-compression of high-energy pulses. To further explore the energy scaling of the proposed scheme, the energy used in section 3.2.1 was increased to 20 mJ and the numerical model was applied to that pulse with $\varepsilon = 15°$ at the input. The geometry ($R = L = 3.5$ m) and the n_2 value (0.57×10^{-21} cm^2 W^{-1}) were changed accordingly. The number of round trips were reduced to 15. The results suggest that the technique is applicable at higher energy levels, too (figure 8). The obtained spectral broadening supports 5.04 fs FTL pulse duration, which corresponds to 2 TW peak power at an efficiency of 50%.

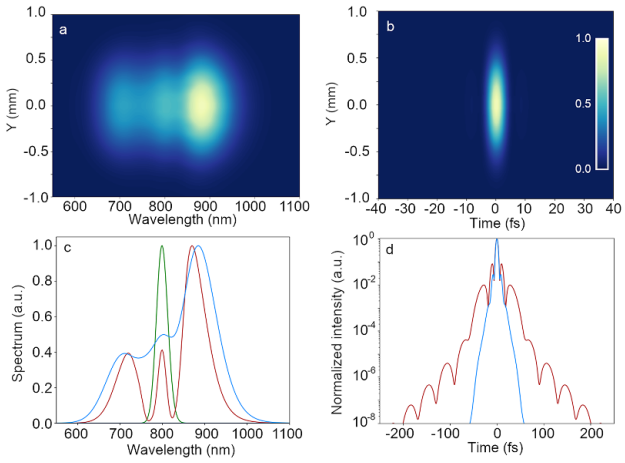

Figure 8. Space integrated spatio-spectral (a) and FTL spatio-temporal profiles (b) of the filtered component. Space integrated spectrum (c): green—input, red—non-filtered and blue—filtered components. Space integrated FTL temporal profiles (d): red—non-filtered and blue—filtered.

4. Conclusions

The simultaneous nonlinear spectral broadening and temporal cleaning of ultrashort pulses in noble gas-filled MPCs have been proposed and investigated by numerical simulations for Yb and Ti:Sa laser systems. We have demonstrated that the technique is suitable for the generation of high contrast, ultrashort pulses with high peak power. At least 10^3 contrast enhancement is feasible independently of the central wavelength or the input energy. Our results show that the input polarization state must be chosen carefully as it highly affects efficiency. Unlike in the case of gradually pumped hollow waveguides [17, 19], where the optimal ellipticity is below 10°, the proposed scheme requires a higher angle. This is probably due to the constant pressure level and the continuously changing beam size. The easy scalability of MPCs makes them a promising candidate for the post-compression of pulses with energies above 100 mJ, which is hardly achievable with waveguides. When the temporal contrast of such high energy pulses is an issue, it can be concurrently improved by exploiting the post-compression and the NER techniques.

Acknowledgments

The ELI-ALPS project (GINOP-2.3.6-15-2015-00001) is supported by the European Union and co-financed by the European Regional Development Fund.

References

[1] Jahn O *et al* 2018 *Optica* **6** 280
[2] Liu J, Okamura K, Kida Y, Teramoto T and Kobayashi T 2010 *Opt. Express* **18** 20645
[3] Hilz P *et al* 2018 *Nat. Commun.* **9** 423
[4] Nagy T, Simon P and Veisz L 2020 *Adv. Phys.* X **6** 1845795
[5] Beetar J E, Gholam-Mirzaei S and Chini M 2018 *Appl. Phys. Lett.* **112** 05112
[6] Chen B, Kretschmar M, Ehberger D, Blumenstein A, Simon P, Baum P and Nagy T 2018 *Opt. Express* **26** 3861–9
[7] Köttig F, Schade D, Koehler J R, Russel P S J and Tani F 2020 *Opt. Express* **28** 9099–110
[8] Hwang S I, Park S B, Mun J, Cho W, Nam C H and Kim K T 2019 *Sci. Rep.* **9** 1613
[9] Lu C, Wu W, Kuo S, Guo J, Chen M, Yang S and Kung A 2019 *Opt. Express* **27** 15638
[10] Hanna M, Délen X, Lavenu L, Guichard F, Zaouter Y, Druon F and Georges P 2017 *J. Opt. Soc. Am.* B **34** 1340–7
[11] Lavenu L, Natile M, Guichard F, Zaouter Y, Délen X, Hanna M, Mottay E and Georges P 2018 *Opt. Lett.* **43** 2252–5
[12] Lavenu L, Natile M, Guichard F, Délen X, Hanna M, Zaouter Y and Georges P 2019 *Opt. Express* **27** 1958–67
[13] Kaumanns M, Kormin D, Nubbemayr T, Pervak V and Karsch S 2021 *Opt. Lett.* **46** 929–32
[14] Kaumanns M, Pervak V, Kormin D, Leschchenko V, Kessel A, Ueffing M, Chen Y and Nubbermeyer T 2018 *Opt. Lett.* **43** 5877–80
[15] Balla P *et al* 2020 *Opt. Lett.* **45** 2572–5
[16] Jullien A *et al* 2005 *Opt. Lett.* **30** 920–2
[17] Kapteyn H C, Murnane M M, Szoke A and Falcone R W 1991 *Opt. Lett.* **16** 490–2
[18] Khodakovskiy N G *et al* 2019 *Laser Phys. Lett.* **16** 095001
[19] Buldt J, Müller M, Klas R, Eidam T, Limpert J and Tünnermann A 2017 *Opt. Lett.* **42** 3761–4
[20] Smijesh N, Zhang X, Fischer P, Muschet A A, Salh R, Tajalli A, Morgner U and Veisz L 2018 *Opt. Lett.* **44** 4028–31
[21] Kalashnikov M P, Risse E, Schönnagel H, Husakou A, Herrmann J and Sandner W 2004 *Opt. Express* **12** 5088–97
[22] Kalashnikov M P, Risse E, Schönnagel H and Sandner W 2005 *Opt. Lett.* **30** 923–5
[23] Cao H, Nagymihály R S, Chvykov V, Khodakovskiy N and Kalashnikov M P 2019 *J. Opt. Soc. Am.* B **36** 2517–25
[24] Börzsönyi Á, Heiner Z, Kalashnikov M P, Kovács A P and Osvay K 2008 *Appl. Opt.* **47** 4856–63
[25] Diels J C and Rudolph W 2006 *Ultrashort Laserpulse Phenomena* 2nd edn (New York: Academic)
[26] Boyd R W 2008 *Nonlinear Optics* 3rd edn (New York: Academic)
[27] Börzsönyi Á, Heiner Z, Kalashnikov M P, Kovács A P and Osvay K 2010 *Opt. Express* **18** 25847–54
[28] Wang D, Leng Y and Xu Z 2013 *Appl. Phys.* B **111** 447–52